

Molecular Structure and Photochemistry of (*E*)- and (*Z*)-Ethyl 3-(2-Indolyl)propenoate. Ground State Conformational Control of Photochemical Behavior and One-Way *E* → *Z* Photoisomerization

Frederick D. Lewis* and Jye-Shane Yang

Department of Chemistry, Northwestern University, Evanston, Illinois 60208-3113

Received: March 26, 1996; In Final Form: June 4, 1996[⊗]

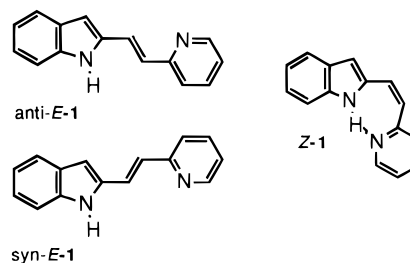
The molecular structure, electronic spectra, and photoisomerization of (*E*)- and (*Z*)-ethyl 3-(2-indolyl)propenoate, two methylated indole derivatives, and their *N,N*-dimethylamide analog have been investigated. The *E* ester exists in the ground state as a mixture of anti and syn rotational isomers. The spectroscopic and photochemical behaviors of the individual anti and syn conformers were characterized with the assistance of comparisons with the behavior of the methylated indole derivatives. The major anti conformer of the *E* ester absorbs and emits at shorter wavelength than the minor syn conformer. The rate constant for singlet state isomerization of the anti conformer is substantially larger than that of the syn conformer, resulting in a shorter singlet lifetime and smaller fluorescence quantum yield for the anti conformer. The behavior of the *E* amide in both the ground and excited states is similar to that of the ester. The *Z* isomers of the ester and amide possess a relatively strong intramolecular hydrogen bond. Their singlet states are weakly fluorescent and photoisomerize inefficiently in nonpolar solvents. Thus photostationary states highly enriched in the *Z* isomers are obtained in nonpolar solvents. The red-shifted, structureless emission observed upon irradiating the *Z* amide in an EPA or methylcyclohexane glass at 77 K is attributed to an excited state tautomer formed via intramolecular hydrogen transfer.

Introduction

A large number of arylethylenes are known to exist as equilibrium mixtures of nearly isoenergetic conformers.^{1–4} In some cases these conformers display sufficiently different spectroscopic properties to permit spectral characterization of the individual conformers. The excited conformers can also differ in their rates of unimolecular isomerization and bimolecular reactions. We recently investigated the molecular structure, spectroscopy, and photochemistry of the *E* and *Z* isomers of 2-(2-(2-pyridyl)ethenyl)indole, **1** (Chart 1), and found that *E*-**1** exists as a mixture of anti and syn conformers which have distinct fluorescence excitation and emission spectra and very different rate constants for photoisomerization.⁴ Furthermore, *Z*-**1** exists as a single conformer due to the presence of an intramolecular hydrogen bond. The singlet state of *Z*-**1** is nonfluorescent and stable with respect to photoisomerization in both nonpolar and polar solvents. While the intramolecular hydrogen bond is clearly implicated in the nonradiative decay of singlet *Z*-**1**, the nonradiative decay pathway has not been elucidated. Photoisomerization of the *E* but not the *Z* isomer results in one-way *E* → *Z* photoisomerization, a relatively rare phenomenon.^{3–7}

The pronounced differences in the spectroscopic properties and photochemistry of the anti and syn conformers of *E*-**1** and the ability of the indole nitrogen to serve as a good hydrogen bond donor make the 2-vinylindoles attractive targets for further investigation. We report here the results of our investigation of the molecular structure, spectra, and photoisomerization of the *E* and *Z* ethyl 3-(2-indolyl)propenoates **2–4**, and the *N,N*-dimethylamide **5** (Chart 2). The methylated indoles **3** and **4** serve as single-conformer models for the anti and syn conformers of **2**, respectively. Whereas the photochemistry of β -arylpropenoate derivatives has been extensively investigated, little is known about the effects of the carboxylate group on the

CHART 1



spectroscopy and photochemistry of the conformers of singlet arylethylenes. The anti and syn conformers of the ester and amide derivatives of 3-(2-naphthyl)propenoic acid are fluorescent; however, strong overlap of the fluorescence spectra prevented dissection of the properties of the anti and syn conformers.^{8,9} The carbonyl groups of esters and amides have previously been found to serve as hydrogen bond acceptors in the *Z* isomers of urocanic acid (3-(4-imidazolyl)propenoic acid) derivatives; however, the absence of fluorescence from either the *E* or *Z* isomers of these and other mononuclear β -arylpropenoic esters and amides prevented a detailed investigation of the photophysics of these molecules.^{6b} We find that the *E* isomers of **2** and **5** exist as mixtures of ground state anti and syn conformers with distinct spectral properties, whereas the *Z* isomers exist predominantly as the anti conformers due to the presence of an intramolecular hydrogen bond. Ground state conformation has a profound effect upon both spectroscopic properties and photochemical behavior.

Results and Discussion

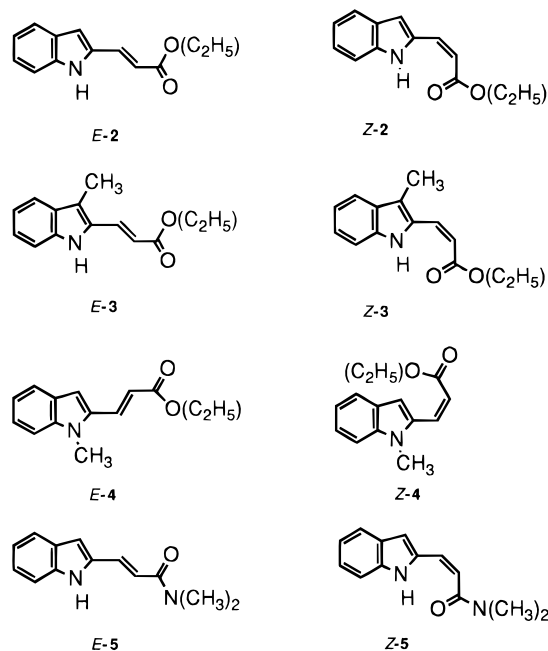
Molecular Structure. The 2-indolylpropenoic acid derivatives **2–5** were prepared from commercial indole starting materials using standard synthetic procedures. The *E* and *Z* isomers are separable by column chromatography and are

[⊗] Abstract published in *Advance ACS Abstracts*, August 1, 1996.

TABLE 1: ^1H NMR and IR Data^a and the Difference in Relative Ground State Energies^b between Z and E Isomers

compd	δ N-H (ppm)	$\nu_{\text{N-H}}$ (cm^{-1})	$\nu_{\text{C=O}}$ (cm^{-1})	$\nu_{\text{C=C}}$ (cm^{-1})	ΔG° (kcal/mol)
E-2	8.49	3471	1695	1634	
Z-2	11.87	3300	1694	1614	-0.7 ± 0.2
E-3	8.58	3478	1689	1626	
Z-3	11.80	3300	1688	1599	0.7 ± 0.1
E-4			1701	1631	
Z-4			1709	1622	> 1.5
E-5	8.76	3467	1648	1596	
Z-5	12.15	3246	1640	1591	-0.9 ± 0.2

^a CDCl_3 solvent for ^1H NMR and CHCl_3 for IR. ^b $\Delta G^\circ = G^\circ(\text{Z}) - G^\circ(\text{E})$.

CHART 2

crystalline solids (except in the case of Z-4 which is an oil) which were purified by recrystallization and fully characterized (see Experimental Section). The existence of intramolecular hydrogen bonds in Z-2, Z-3, and Z-5 was established by ^1H NMR and IR spectroscopies. Downfield chemical shifts of N-H (> 3 ppm) and lower N-H stretching frequencies (> 170 cm^{-1}) are observed in comparison to the values for the corresponding E isomers (Table 1). The larger downfield chemical shift and the smaller $\nu_{\text{N-H}}$ observed for Z-5 vs Z-2 indicate that the amide group behaves as a slightly stronger hydrogen bond acceptor than the ester group.

The ground state conformations of 2-5 have been investigated by both experimental and computational methods. The E isomers of 2-5 can adopt any of four planar conformations as a consequence of rotation about the vinyl-indole and enone single bonds. The relative intensities of infrared $\nu_{\text{C=C}}$ vs $\nu_{\text{C=O}}$ bands can be employed to assign the enone conformations.¹⁰ By analogy to our previous studies of cinnamate ester and amide conformation,¹¹ the IR data are consistent with s-trans enone conformations for esters E-2-E-4 and s-cis for amide E-5 (Chart 2). The hydrogen-bonded conformers of Z-2, Z-3, and Z-5 have, of necessity, s-cis enone conformations.

NOE difference experiments for E-2-E-4 in CDCl_3 solution and for E-2 in $\text{DMSO-}d_6$ solution were carried out to provide information about their vinyl-indole conformations. The results are depicted in Figure 1. Two irradiation frequencies were used in each case: one at the frequency absorbed by indole N₁-H

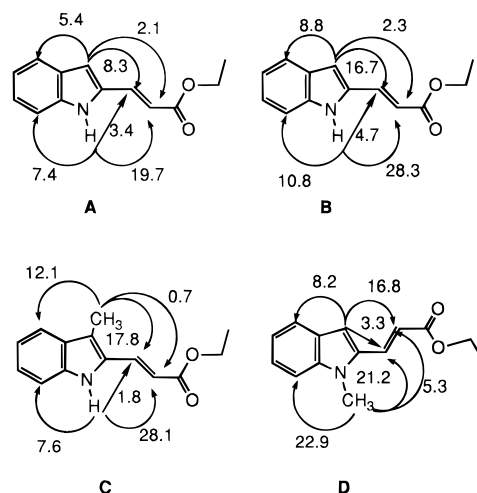


Figure 1. NOE data (%) for (E)-ethyl 3-(2-indolyl)propenoate (E-2) in CDCl_3 (A) and $\text{DMSO-}d_6$ (B), (E)-ethyl 3-(3-methyl-2-indolyl)propenoate (E-3) in CDCl_3 (C), and (E)-ethyl 3-(N-methyl-2-indolyl)propenoate (E-4) in CDCl_3 (D).

(or N₁-CH₃) and the other by indole C₃-H (or C₃-CH₃). NOE data indicate that the lowest energy vinyl-indole conformations are those shown in Figure 1. The observed vinyl-indole conformations for E-3 and E-4 are consistent with the anticipated effect of nonbonded repulsion between the methyl substituent and the vinyl group.^{4,12} The NOE data for E-2 more closely resemble that for E-3 than for E-4. On this basis we conclude that the major and minor conformers of E-2 are anti and syn, respectively. The larger NOE values observed for E-2 in $\text{DMSO-}d_6$ vs CDCl_3 may reflect a difference in solvent viscosity, and the larger values for E-3 and E-4 vs E-2 in CDCl_3 may reflect a reduction in rotational rates upon methylation.¹³

The gas phase conformational energies of the four possible conformers of E-2-E-5 were calculated using the MM2 force field.¹⁴ In accord with IR assignment, the two s-trans enone conformations have lower energy by 2.4 ± 0.2 kcal/mol than the s-cis conformations in the cases of E-2-E-4, whereas the two s-cis enone conformations of E-5 are more stable by 2.3 ± 0.2 kcal/mol than the s-trans conformations. In addition, the two lower energy conformers in E-2 and E-5 are nearly isoenergetic ($\Delta G = 0.2 \pm 0.2$ kcal/mol), but only one lowest energy conformer exists in the cases of E-3 and E-4 ($\Delta G > 1.2 \pm 0.2$ kcal/mol). These calculations do not rule out the possible presence of higher energy conformations of E-2-E-5 in solution.¹⁵

The difference in relative ground state energies between E and Z isomers of 2-5 in benzene solution was determined by free-radical-initiated isomerization using irradiation of either iodine or diphenyl diselenide as the radical source (Table 1).¹⁶ Z-2 and Z-5 are more stable than their corresponding E isomers by ~ 0.8 kcal/mol, as is the case for Z-1 ($\Delta G = 0.2$ kcal/mol in benzene solution⁴). In contrast, Z-4, which is incapable of forming an intramolecular hydrogen bond, is less stable than its E isomer by > 1.5 kcal/mol. Z-3 is less stable than its E isomer by 0.7 kcal/mol, in spite of the existence of an intramolecular hydrogen bond. The nonbonded interaction between the 3-methyl substituent and the vinyl hydrogen (A^(1,3) strain¹²) may be larger for the more planar Z isomer vs the E isomer. Clearly there is no simple relationship between the relative thermodynamic stability of the Z vs E isomer and the N-H chemical shift or vibrational frequency.

Absorption Spectra. The electronic absorption spectra of E and Z isomers of 2-4 in hexane solution are shown in Figure 2. The appearance of absorption spectra of E-5 and Z-5 (not

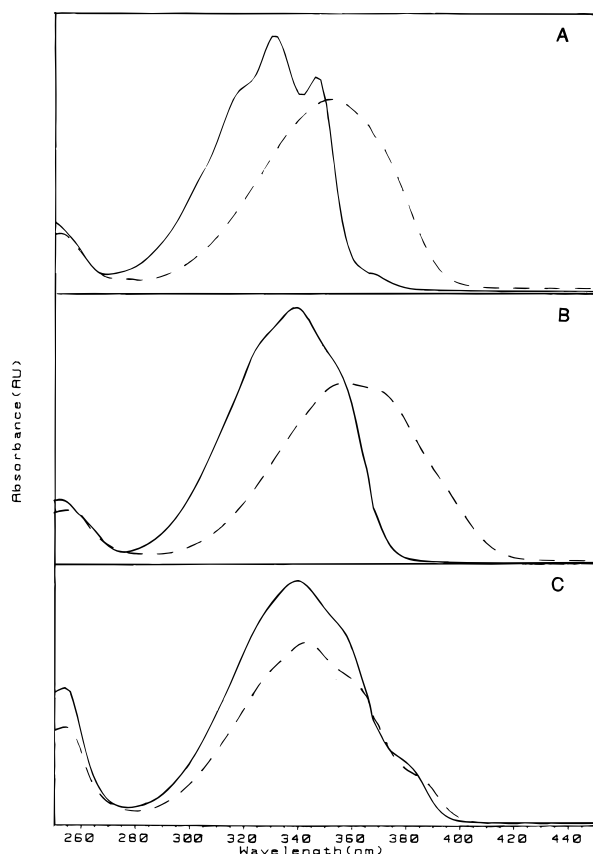


Figure 2. UV spectra of (*E*)- (—) and (*Z*)- (---) ethyl 3-(2-indolyl)propenoate (**2**) (A), ethyl 3-(3-methyl-2-indolyl)propenoate (**3**) (B), and ethyl 3-(*N*-methyl-2-indolyl)propenoate (**4**) (C) in hexane solution.

TABLE 2: Absorption and Fluorescence Spectral Data

compd	solvent	$\lambda_{\text{max,abs}}$ (nm)	ϵ_{max}	$\lambda_{\text{max,fl}}$ (nm)
<i>E</i> -2	C ₆ H ₁₄	330, 346	32 200, 27 200	379, 400
	EtOH	340	31 500	449
<i>Z</i> -2	C ₆ H ₁₄	352		
	EtOH	348	22 300	
<i>E</i> -3	C ₆ H ₁₄	340	26 400	380, 397
	EtOH	350	28 700	438
<i>Z</i> -3	C ₆ H ₁₄	356	24 600	
	EtOH	356	26 700	
<i>E</i> -4	C ₆ H ₁₄	340	26 600	397, 417
	EtOH	344	23 600	458
<i>Z</i> -4	C ₆ H ₁₄	342	19 700	
	EtOH	342	18 700	
<i>E</i> -5	C ₆ H ₁₄	330, 346		378, 398
	EtOH	340	34 100	433
<i>Z</i> -5	C ₆ H ₁₄	348		
	EtOH	342	22 100	

shown) are very similar to those of *E*-2 and *Z*-2, respectively. The absorption maxima of hydrogen-bonded *Z* isomers (*Z*-2, *Z*-3, and *Z*-5) are at longer wavelengths than those of their *E* isomers in both nonpolar and polar solvents (Table 2). In contrast, the absorption maximum of *Z*-4, which does not possess an intermolecular hydrogen bond, is similar to that of *E*-4. The effect of conformation upon the absorption spectra of β -substituted styrenes has been discussed by Fueno et al.¹⁷ They observed that planar *Z* isomers absorb at lower energy than the corresponding *E* isomers, whereas nonplanar *Z* isomers absorb at higher energy. Intramolecular hydrogen bonding may favor a more nearly coplanar geometry for the vinylindole chromophores in *Z*-2, *Z*-3, and *Z*-5 than in their *E* isomers or in *Z*-4. Methylation on the indole C₃ or N₁ positions results in a small red-shift in the absorption maximum (5–10 nm) and a loss of vibrational structure (Figure 2). Increasing solvent

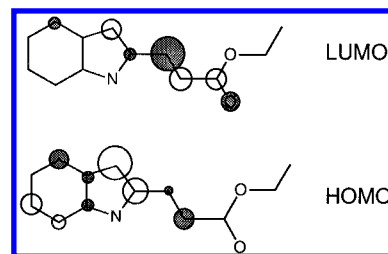


Figure 3. ZINDO-calculated highest occupied and lowest unoccupied molecular orbitals for (*E*)-ethyl 3-(2-indolyl)propenoate (*E*-2).

polarity also results in loss of vibrational structure and a red-shift of the absorption maximum (Table 2).

The electronic structure and spectra of *syn-E*-2, *anti-E*-2, and the *Z*-2 have been investigated by means of semiempirical INDO/S-SCF-CI (ZINDO) calculations using the algorithm developed by Zerner and co-workers.¹⁸ The conformations of molecules for calculation are adopted from the results of MM2 optimization. The ZINDO-derived highest occupied molecular orbital (HOMO) and the lowest unoccupied molecular orbital (LUMO) for *anti-E*-2 are shown in Figure 3. The HOMO is localized on the vinylindole portion of the molecule and the LUMO on the enone portion of the molecule. Thus the ester and amide are expected to have similar electronic structures, in accord with their similar absorption spectra. The energy of the HOMO is well separated energetically from that of the two lower energy π -bonding orbitals and the nonbonding orbital. The first allowed transitions for *syn-E*-2, *anti-E*-2, and *Z*-2 are all calculated to be of relatively pure and allowed HOMO \rightarrow LUMO, $\pi \rightarrow \pi^*$ character. The ZINDO calculated frontier orbitals and singlet states of *syn-E*-2, *anti-E*-2, and the *Z*-2 are provided as supporting information.

The calculated transition energies and oscillator strengths are in the order *anti-E*-2 (314 nm, $f = 0.88$) > *syn-E*-2 (321 nm, $f = 0.76$) > *Z*-2 (337 nm, $f = 0.50$). The longer wavelength and lower oscillator strength for *Z*-2 vs *E*-2 are in agreement with the observed spectra (Figure 2). In addition to the allowed $\pi \rightarrow \pi^*$ transition, ZINDO calculations indicate the presence of $n \rightarrow \pi^*$ transitions of very low oscillator strength (0.001–0.005) at energies below their lowest $\pi \rightarrow \pi^*$ transitions by ~ 2700 cm⁻¹. The n, π^* states have extensive configuration interaction involving all of the low-energy π^* orbitals. Similar results have been obtained from ZINDO calculations for 2-naphthylpropenoic acid derivatives.⁹ It has been noted that ZINDO may not provide reliable energies for n, π^* states in such cases.¹⁹ On the basis of the fluorescence properties described in the following section, it seems likely that the *E* isomers of **2–5** all possess lowest energy π, π^* singlet states.

Excited State Behavior of the *E* Isomers. The fluorescence emission and excitation spectra of *E*-2 in hexane solution bubbled with nitrogen or oxygen are shown in Figure 4a. Oxygen has little effect on the appearance of the emission spectrum but reduces the intensity of the long wavelength band of the excitation spectrum. This selective quenching is indicative of the presence of two fluorescent species with different excitation spectra and lifetimes. A synchronous scan ($\lambda_{\text{em}} - \lambda_{\text{ex}} = 10$ nm) of the fluorescence spectrum for a highly dilute hexane solution of *E*-2 is shown in Figure 5. The appearance of two distinct bands at 346 and 366 nm provides further evidence for the presence of two fluorescing species.²⁰ The ratio of band intensities (366/346 nm ~ 6) does not change at lower concentrations, indicating that reabsorption of emitted light is not influencing this ratio.

Fluorescence quantum yield (Φ_F) and lifetime data for *E*-2 obtained in several solvents at room temperature are reported

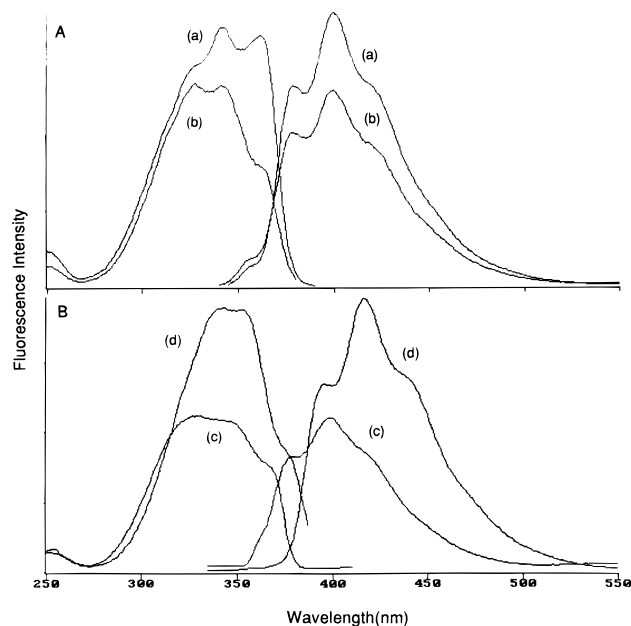


Figure 4. Fluorescence emission and excitation spectra of (A) (*E*)-ethyl 3-(2-indolyl)propenoate (*E*-2) in hexane solution bubbled with nitrogen (a) and oxygen (b) ($\lambda_{\text{ex}} = 330$ nm and $\lambda_{\text{em}} = 400$ nm) and (B) (*E*)-ethyl 3-(3-methyl-2-indolyl)propenoate (*E*-3) ($\lambda_{\text{ex}} = 325$ nm and $\lambda_{\text{em}} = 420$ nm) (c) and (*E*)-ethyl 3-(*N*-methyl-2-indolyl)propenoate (*E*-4) ($\lambda_{\text{ex}} = 325$ nm and $\lambda_{\text{em}} = 397$ nm) (d) in hexane solution bubbled with nitrogen.

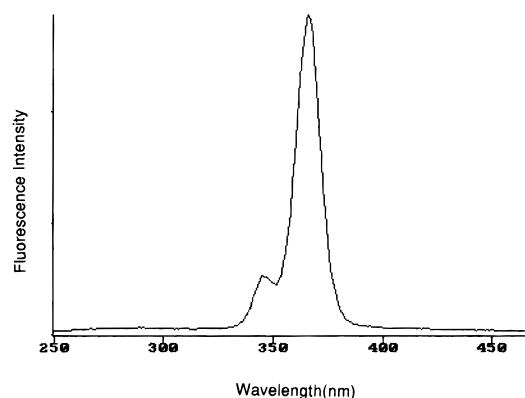


Figure 5. Fluorescence synchronous scan ($\lambda_{\text{em}} - \lambda_{\text{ex}} = 10$ nm) of (*E*)-ethyl 3-(2-indolyl)propenoate (*E*-2) in hexane solution.

in Table 3. Dual exponential fluorescence decays are observed in all solvents. The decay times for the shorter-lived component of *E*-2 are near the time resolution of our instrument and thus should be viewed as approximate ($0.1 < \tau_2 < 0.3$ ns). The dependence of preexponentials of the fluorescence decay of *E*-2 in hexane on excitation and emission wavelengths was also investigated. When the solution is excited at 322 nm and the emission decay is detected at 358 nm, emission from the short-lived component has the larger preexponential. In contrast, emission from the long-lived component has the larger preexponential when the excitation and emission wavelengths are 362 and 419 nm, respectively (Table 3). On the basis of the above observations, the short-lived and long-lived components can be assigned to species with shorter and longer wavelength 0,0 bands, respectively. Both the appearance of the fluorescence spectrum and the lifetimes for *E*-2 are similar to those previously reported for *E*-1,⁴ in accord with the assignment of the lowest singlets to vinyl-indole π,π^* states.

The use of arene methylation to “lock” a vinylarene into a single conformer has been successfully employed in previous investigations of rotational isomers.^{2,4,21} On the basis of these

TABLE 3: Fluorescence Quantum Yields (Φ_{F}) and Lifetime Data (τ) with Preexponential Values (A) at Room Temperature

compd	solvent	λ_{ex}^a	Φ_{F}	$\tau_{1,\text{ns}}$	A_1	% ^b	$\tau_{2,\text{ns}}^c$	A_2	% ^b
<i>E</i> -2	C_6H_{14}	322		1.4	0.09	52	0.13	0.91	48
		362		1.3	0.54	90	0.17	0.46	10
	PhH	338	0.030						
	CH_3CN	334	0.048	1.1	0.45	76	0.29	0.55	24
	DMSO	342	0.037						
	EtOH	340	0.028	0.85	0.59	87	0.19	0.41	13
<i>E</i> -3	PhH	EPA ^d	336	4.0	0.30	40	2.6	0.70	60
		348	0.013	0.52	1.00	100			
<i>E</i> -4	PhH	348	0.0040						
		346	0.26	2.47	1.00	100			
<i>E</i> -5	PhH	346	0.086	1.35	1.00	100			
		336	0.051						
		CH_3CN	330	0.033	1.0	0.53	80	0.28	0.47
	DMSO	338	0.036						

^a Excitation wavelength corresponding to the maximum in the fluorescence excitation spectrum used for both fluorescence quantum yield and lifetime measurements. ^b Contribution to total fluorescence decay [$A_1\tau_1$ or $A_2\tau_2/(A_1\tau_1 + A_2\tau_2)$]. ^c Decay times < 0.3 ns are near the time resolution of our instrumentation and are considered approximate (± 0.1 ns). ^d Data obtained at 77 K.

precedents, *E*-3 and *E*-4 were expected to serve as single-conformer models for *anti-E*-2 and *syn-E*-2, respectively. The fluorescence emission and excitation spectra of *E*-3 and *E*-4 in hexane solution are shown in Figure 4B. Both display a vibrational structure similar to that for *E*-2. Except for the absence of the shoulder at the onset of the emission spectrum, the vibrational bands of *E*-3 overlap with those of *E*-2. The vibrational bands of *E*-4 are shifted by ~ 20 nm to the red, and thus its 0–0 band lies at the same position as the 0–1 band of *E*-3. Single-exponential decays are observed for *E*-3 and *E*-4 in both benzene and ethanol. *E*-3 exhibits lower values of Φ_{F} and shorter lifetimes than those for *E*-4 (Table 3).

Correlation of the behavior of *E*-3 and *E*-4 with that of *E*-2 suggests that *syn-E*-2 absorbs and emits at longer wavelength with larger fluorescence yield and longer lifetime than *anti-E*-2. This assignment is consistent with the selective quenching of the long-wavelength fluorescence excitation band by oxygen (Figure 4A) and with the effect of excitation and emission wavelength on the preexponentials for fluorescence decay (Table 3). The low total fluorescence quantum yields observed for *E*-2 (Table 3) indicate that *anti-E*-2 is the major conformer, in accord with the NOE experiments for *E*-2 (Figure 1). Increasing solvent polarity results in red-shifted (Table 2) and broadened fluorescence spectra for *E*-2–4. The fluorescence quantum yields for both *E*-3 and *E*-4 are lower in ethanol than in benzene solution. The fluorescence quantum yields and lifetimes of *E*-2 display only minor variation with solvent (Table 3).

Quantum yields for photoisomerization of *E*-2–*E*-4 ($\Phi_{\text{E,Z}}$) are reported in Table 4. The significantly higher value for *E*-3 vs *E*-4 indicates that the shorter lifetime of *E*-3 is due, at least in part, to more rapid isomerization. The value of $\Phi_{\text{E,Z}}$ for *E*-2 is even higher than that for *E*-3, in accord with our assignment of the anti conformation to the short-lived major conformer. The values of $\Phi_{\text{E,Z}}$ for *E*-2–*E*-4 decrease with increasing solvent polarity. The decrease in $\Phi_{\text{E,Z}}$ for *E*-2 might be attributed to a decrease in the population of the reactive anti conformer in more polar solvents; however, NOE data indicate that the conformer populations are similar in CDCl_3 and DMSO solution. Furthermore, increasing solvent polarity also results in a decrease in the isomerization quantum yields of *E*-3 and *E*-4 which exist as single conformers. The solvent dependence of $\Phi_{\text{E,Z}}$ for *E*-2–*E*-4 is similar to that previously observed for the photoisomerization of 3-(2-pyridyl)propenamides.⁵ Solvation of the polar

TABLE 4: Quantum Yields for Isomerization and Isomer Content for the Photostationary States^a

compd	solvent	$\Phi_{E,Z}$	$\Phi_{Z,E}$	%Z ^b
2	PhH	0.65	0.047	95
	CH ₃ CN	0.61	0.10	72
	DMSO	0.37	0.19	51
	EtOH	0.22	0.073	67
3	PhH	0.47	0.02	98
	EtOH	0.06	0.005	68
4	PhH	0.034	0.34	<22 ^c
	EtOH	0.012	0.12	<20 ^c
5	PhH	0.77	0.0049	98
	CH ₃ CN	0.60	0.056	96
	DMSO	0.25		82
	EtOH	0.30		85

^a Excitation wavelength is 313 nm. ^b Same results obtained starting with either pure *E* or pure *Z* isomers. ^c Compound not very stable upon prolonged irradiation.

TABLE 5: Summary of Ground and Excited State Properties of Conformers *anti-E-2* and *syn-E-2* and Model Compounds *E-3* and *E-4* in Nonpolar Solvent at Room Temperature

	<i>anti-E-2</i>	<i>syn-E-2</i>	<i>E-3</i>	<i>E-4</i>
τ , ns	~ 0.2	1.0	0.52	2.5
Φ_F	0.006 ± 0.003	0.11 ± 0.03	0.013	0.26
k_f , × 10 ⁻⁸ s ⁻¹ ^a	0.3 ± 0.2	1.1 ± 0.2	0.25	1.0
ΔG° , kcal/mol ^b	0	0.8 ± 0.2		
Es, kcal/mol ^c	80	76	75	72
$\Phi_{E,Z}$	0.83 ± 0.2	0.06 ± 0.02	0.47	0.034
k_i , × 10 ⁻⁸ s ⁻¹ ^a	42 ± 20	0.6 ± 0.2	9.0	0.13

^a Estimated errors for *anti-E-2* are larger than those for *syn-E-2* due to its short lifetime (Table 3, footnote c). ^b Free energies relative to *anti-E-2* estimated from experimental data in hexane or benzene solutions. ^c Singlet energies estimated from emission spectra in hexane solution.

amide or ester group might result in a solvent-induced barrier for photoisomerization.

The ground and excited state properties of conformers *syn-E-2* and *anti-E-2* and of their single conformer models *E-3* and *E-4* in nonpolar solvent are summarized in Table 5. The ground state conformer populations *E-2* are estimated to be 77% *anti* and 23% *syn* in nonpolar solvents, on the basis of the 1:6 ratio of peak intensities in the synchronous scan spectrum (Figure 5) and the assumption that the fluorescence quantum yield ratio for the conformers is the same as that for the single-conformer models *E-3* and *E-4* (Table 3). These estimated populations are consistent with the NOE data (Figure 1) and can be used with the measured value of Φ_F for *E-2* to obtain approximate values of $\Phi_F = 0.006$ for *anti-E-2* and 0.11 for *syn-E-2*. Similarly, these populations can be used with the measured quantum yields for isomerization of *E-2*–*E-4* to obtain approximate values of $\Phi_{E,Z} = 0.83$ for *anti-E-2* and 0.06 for *syn-E-2*.

Values of k_f and k_i for the *anti* and *syn* conformers of *E-2* and for *E-3* and *E-4* can be calculated from the estimated or measured quantum yields and singlet lifetimes (Table 5). Values of k_i are not corrected for possible partitioning of a twisted intermediate between *E* and *Z* isomers. The estimated errors are largest in the case of *E-2* because of possible errors in the measurement of its short singlet lifetime as well as in estimation of the quantum yields. The smaller value of k_f and larger value of k_i for the *anti* vs *syn* conformer of *E-2* parallel the differences observed for *E-3* vs *E-4*. The larger values of k_i for *anti* vs *syn-E-2* and for *E-3* vs *E-4* plausibly reflect the higher singlet energies of the more reactive conformational or geometric isomer, which could result in a lower barrier for twisting about the double bond. Similarly, the larger values of k_i for *anti-E-2*

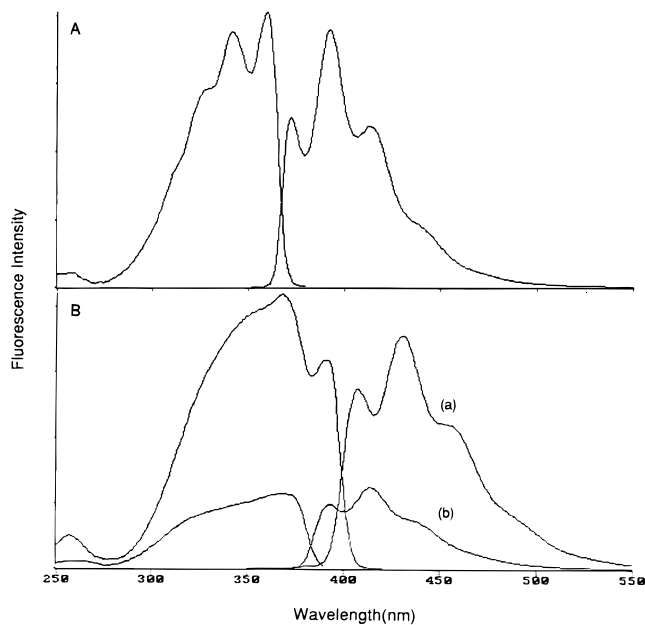


Figure 6. Fluorescence emission and excitation spectra of (A) (*E*)-ethyl 3-(2-indolyl)propenoate (*E-2*) ($\lambda_{ex} = 342$ nm and $\lambda_{em} = 392$ nm) and (B) (*E*)-ethyl 3-(3-methyl-2-indolyl)propenoate (*E-3*) ($\lambda_{ex} = 320$ nm and $\lambda_{em} = 400$ nm) (a) and (*E*)-ethyl 3-(*N*-methyl-2-indolyl)propenoate (*E-4*) ($\lambda_{ex} = 342$ nm and $\lambda_{em} = 434$ nm) (b) in EPA at 77 K.

vs *E-3* and *syn-E-2* vs *E-4* may reflect the lower singlet energies of the methylated indoles. It is interesting to note that the values of k_f for *anti-E-2* and *E-3* and for *syn-E-2* and *E-4* are essentially identical. Thus methylation of the indole nucleus results in a decrease in the singlet energy and isomerization rate constant but has little effect upon either the fluorescence rate constant or the vibronic structure.

The spectroscopy, photophysical, and photochemical behavior of *E-5* are all similar to those of *E-2*. Thus the difference in enone conformation (*s-trans* for *E-2* and *s-cis* for *E-5*) has no noticeable consequences. This result is in accord with the results of ZINDO calculations for *E-2* (Figure 2 and supporting information), which indicate that the HOMO and LUMO are largely localized on the vinylindole portion of the molecule.

The fluorescence spectra of *E-2*–*4* in EPA glasses formed by slow cooling to 77 K are shown in Figure 6. The spectra of *E-3* and *E-4* display enhanced vibrational resolution and are red-shifted by ~12 nm (Figure 6B) compared to their room temperature spectra in hexane solution (Figure 4A). The 77 K spectrum of *E-2* (Figure 6A) is assigned to the *anti* conformer on the basis of the simple mirror image relationship between the excitation and emission spectrum and the 14 nm red-shift of the 0,0 band compared to the room temperature spectrum in hexane solution. Increases in the population and singlet lifetime of the *anti* conformer upon cooling evidently result in its domination of the total emission spectrum. The fluorescence decay of *E-2* at 77 K is, however, biexponential with decay times of 4.0 and 2.6 ns. The observation of dual exponential decay from a single conformer can be attributed to the formation of different solvent domains upon cooling the mixed solvent EPA.²² Different solvent domains could also account for minor variations in the fluorescence excitation and emission spectra of *E-2* in EPA at 77 K that are observed when the emission or excitation wavelength is changed.

Excited State Behavior of the *Z* Isomers. The *Z* isomers of 2–5 are all very weakly fluorescent at room temperature in solution. In the case of *Z-4* the room temperature fluorescence is dominated by a 2–3% residual impurity of *E-4*. Quantum

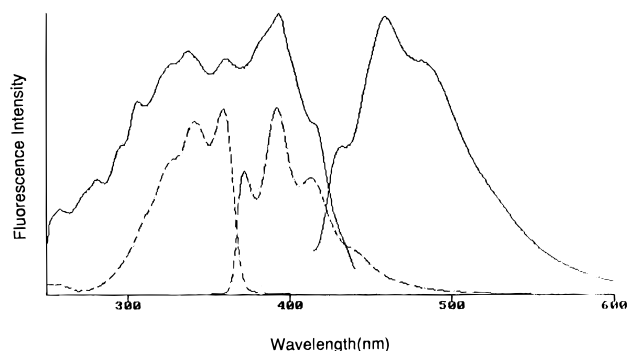


Figure 7. Fluorescence emission and excitation spectra of (Z)-ethyl 3-(2-indolyl)propenoate (Z-2) in EPA at 77 K ($\lambda_{ex} = 394$ nm and $\lambda_{em} = 458$ nm). Spectra of (E)-ethyl 3-(2-indolyl)propenoate (E-2) (---) are included for purposes of comparison.

yields for photoisomerization of Z-2–Z-5 ($\Phi_{Z,E}$) are reported in Table 4. The values of $\Phi_{Z,E}$ for Z-2, Z-3, and Z-5 in nonpolar solvents are all very small (<0.05). Since the quantum yields for isomerization of the corresponding E isomers are relatively large, the photostationary states are enriched in the Z isomers (Table 4). In the case of **4** the value of $\Phi_{Z,E}$ is significantly larger than that for $\Phi_{E,Z}$ in nonpolar solvents, and the photostationary state is enriched in the E isomer. The much larger values of $\Phi_{Z,E}$ for Z-4 compared to those for Z-2, Z-3, and Z-5 can be attributed to the absence of an intramolecular hydrogen bond for the former molecule. Highly inefficient photoisomerization has previously been observed for Z-1⁴ and several other molecules possessing intramolecular hydrogen bonds.^{5,6} The intramolecular hydrogen bond may either inhibit twisting about the double bond or introduce competing nonradiative decay pathways, including intramolecular hydrogen transfer.

The values of $\Phi_{Z,E}$ for Z-2 and Z-5 are larger in polar, aprotic solvents than in benzene, resulting in a decrease in the Z isomer content of the photostationary state. Polar solvents might disrupt the intramolecular hydrogen bond as previously observed for the 3-(2-pyridyl)propenamides,⁵ but not for Z-1.⁴ The low values of $\Phi_{Z,E}$ for Z-2–Z-4 in ethanol solution may reflect a solvent-induced barrier for isomerization, as proposed for the E isomers.

The fluorescence excitation and emission spectra of Z-2 at 77 K in an EPA glass are shown in Figure 7, along with the spectra of E-2. Excitation at 394 nm, a wavelength absorbed by Z-2 but not *anti*-E-2, results in a broad spectrum with poorly resolved vibrational structure and a 0,0 band at 431 nm. The red-edge of the excitation spectrum is in the same spectral region as the long-wavelength tail of the room temperature absorption spectrum of Z-2 (Figure 2). Excitation at 342 nm, a wavelength absorbed by both E-2 and Z-2, results in overlapping emission from both isomers. Since E-2 is more strongly fluorescent than Z-2 in the glass as well as in solution, trace amounts of E-2 which are either present initially or formed via photoisomerization in the glass can account for the observation of emission from E-2. Repeated scanning results in a growth of E-2 fluorescence, indicating that isomerization of Z-2 does occur in the glass.

The fluorescence excitation and emission spectra of Z-5 at 77 K in an EPA glass are shown in Figure 8. Similar spectra were obtained in a nonpolar methylcyclohexane glass. The maximum in the excitation spectrum of Z-5 is at shorter wavelength than that for Z-2 (376 vs 394 nm); however, the emission spectrum of Z-5 is broadened and substantially red-shifted compared to that of Z-2 (Figure 7). The strongly red-shifted fluorescence of Z-5 may result from adiabatic intramolecular hydrogen transfer resulting in the formation of the

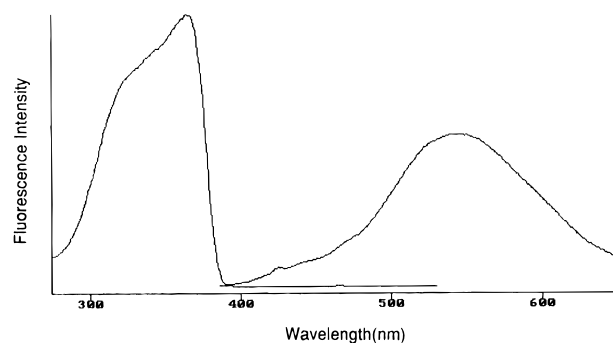


Figure 8. Fluorescence emission and excitation spectra of (Z)-N,N-dimethyl-3-(2-indolyl)propenamamide (Z-5) in EPA at 77 K irradiated at $\lambda_{ex} = 363$ nm and monitored at 546 nm.

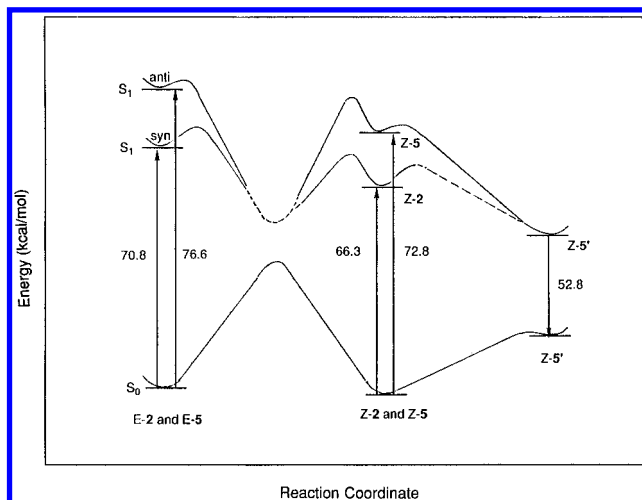
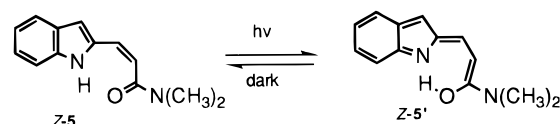


Figure 9. Schematic potential energy surfaces for the singlet state photoisomerization and hydrogen transfer of (E) and (Z)-ethyl 3-(2-indolyl)propenoate (**2**) and N,N-dimethyl-3-(2-indolyl)propenamamide (**5**).

CHART 3



fluorescent tautomer Z-5' (Chart 3). Adiabatic formation of a fluorescent tautomer has been observed both at room temperature and at 77 K for other arylenes possessing intramolecular hydrogen bonds.^{3,6} Tautomerization may account for the low value of $\Phi_{Z,E}$ as well as the absence of fluorescence from Z-5 in solution or the glass. The observation of structured fluorescence from Z-2 but tautomer fluorescence from Z-5' suggests that the tautomerization process may be more favorable for singlet Z-5. One possible explanation for this difference is the higher singlet energy for Z-5 vs Z-2 estimated from the 0,0 bands of their fluorescence excitation spectra.

Concluding Remarks. The results of our investigation of the structure and photochemical behavior of the E and Z isomers of **2** and **5** can be summarized using the potential energy diagram in Figure 9. Both E-2 and E-5 exist as mixtures of two ground state conformers, which are *anti* (major) or *syn* (minor) with respect to rotation about the vinyl–indole bond and have the same enone conformation (*s-trans* for E-2 and *s-cis* for E-5). The methylated indoles E-3 and E-4 provide single-conformer models for *anti*-E-2 and *syn*-E-2, respectively. The excited state behaviors of the *anti* conformers of E-2 and E-5 are similar to that of E-3, but quite different from that of the *syn* conformers or E-4. The lower singlet energies of the *syn* conformers (Figure 9) are consistent with the results of ZINDO

calculations. Photoisomerization of the anti conformers and *E-3* is ~ 70 times faster than for the syn conformers or *E-4*, resulting in shorter lifetimes and lower fluorescence quantum yields for the anti conformers. Faster isomerization may be attributed to the higher singlet energies of the anti conformers.

The *Z* isomers of **2**, **3**, and **5** exist as single ground state conformers which possess a strong intramolecular hydrogen bond. The *Z* isomers are very weakly fluorescent and have low photoisomerization quantum yields in nonpolar solution. Their singlet energies (Figure 9) can be estimated from fluorescence excitation spectra in low-temperature glasses. The lower singlet energy of *Z-2* vs *E-2* is consistent with the results of ZINDO calculations (supporting information). The low-temperature fluorescence of *Z-2* and *Z-5* are assigned to the singlet of *Z-2* and the tautomer of *Z-5*, respectively. The occurrence of tautomerization for *Z-5* but not *Z-2* may reflect the higher singlet energy of *Z-5* (Figure 9).

These results provide the first detailed information about the effects of β -carboxylate substituents on the spectroscopy and photochemistry of the conformational isomers of an arylolethylene. The photophysical properties of the anti and syn conformers of *E-2* and *E-5* in nonpolar solvents are quite similar to those of the diarylethylene *E-1*.⁴ A β -carboxylate substituent significantly shortens the singlet lifetimes of vinylanthracene⁹ and styrene¹¹ due to the introduction of a low-energy n,π^* singlet state. This is not the case for the vinylindoles *E-2* and *E-5* which have lowest energy π,π^* excited states. Since the lowest singlet states of *E-1*, *E-2*, and *E-5* are localized on the vinylindole portion of the molecule, it is not surprising that the behavior of the excited state is more dependent upon vinylindole conformation (anti or syn) than the enone conformation (*s-trans* for *E-2* and *s-cis* for *E-5*). Thus the presence of alternate ground state enone conformers (*s-cis* for *E-2* and *s-trans* for *E-5*) may have gone undetected in our fluorescence decay measurements.

The β -carboxylate substituent has a more pronounced effect on the structure and behavior of the *Z-2* and *Z-5* than on their *E* isomers due to the presence of an intramolecular hydrogen bond. The observation of red-shifted fluorescence from *Z-5* in a low-temperature glass indicates that excited state hydrogen transfer followed by return transfer in the ground state provides a pathway for nonradiative decay which may be responsible for the inefficient photoisomerization of the *Z* isomers in solution. In view of the polar nature of the ester and amide groups, it is not surprising that the behavior of both the *E* and *Z* isomers of **2** and **5** is strongly solvent dependent.

Experimental Section

General Methods. ¹H NMR and ¹³C NMR (proton-decoupled) spectra were recorded using a Varian Gemini 300 spectrometer. NOE experiments were performed with a Varian Unity Plus 400 spectrometer using samples degassed by four freeze-pump-thaw cycles. Elemental analyses were performed by Oneida Research Services Inc., Whitesboro, NY. UV-vis absorption spectra were recorded using a Hewlett-Packard 8542A diode array spectrophotometer in 1 cm path length quartz cuvettes. Infrared spectra of ca. 0.01 M solutions were recorded on a Mattson FT-IR spectrometer. Mass spectra were determined with a Hewlett-Packard 5985 GC/VG Analytical 70-250SE MS system using an ionizing voltage of 70 V. Melting points were determined on a Fisher-Johns melting point apparatus.

Fluorescence spectra of degassed solutions were recorded with a Spex Fluoromax spectrometer. Low-temperature emission spectra and fluorescence spectra were obtained using a liquid nitrogen cooled fluorescence Dewar with a hanging finger

window or Oxford Instruments variable temperature liquid nitrogen cryostat model DN1704 equipped with a model ITC4 temperature controller. Fluorescence quantum yields were determined relative to equiabsorbing solutions of pyrene ($\Phi_F = 0.60$ in nonpolar and 0.53 in polar solvent^{23a}), anthracene ($\Phi_F = 0.27$ in nonpolar and polar solvent^{23a}), or 2,5-bis(5-*tert*-butyl-2-benzoxazolyl)thiophene (BBOT, $\Phi_F = 0.67$ ^{23b,c}) in methylcyclohexane. Fluorescence decays were obtained on a Photon Technology International LS-1 single-photon-counting apparatus with a gated hydrogen arc lamp (time resolution ~ 0.2 ns) using a scatter solution to approximate the lamp decay. Decays were analyzed using deconvolution and single- or multiexponential least-squares fitting as described by James et al.²⁴ The goodness of the fit was judged by the reduced χ^2 value (< 1.2 in all cases), the randomness of the residuals, and the autocorrelation function.

Photoisomerization quantum yields and *E,Z* photoequilibria were determined for 2 mL aliquots of 0.005 M solutions of esters or amides contained in 1 cm path length quartz cuvettes sealed with white rubber septa and purged for 5–10 min with dry nitrogen. Samples were irradiated in triplicate with light from the Oriel Optical bench equipped with a 200 W high-pressure mercury-xenon lamp and a Bausch and Lomb high-intensity monochromator set at 313 nm. Quantum yields were analyzed for isomer formation at less than 10% conversion with *trans*-stilbene as the actinometer.²⁵ Product ratios were analyzed with Hewlett-Packard 5890A Chromatograph equipped with 10 m \times 0.53 mm capillary columns coated with poly(dimethylsiloxane) or poly(methylphenylsiloxane). Ground state thermal equilibria were determined by irradiating benzene solutions of **2**, **3**, and **4** containing a few iodine crystals with an incandescent lamp or by irradiation of benzene solutions of **5** and diphenyl diselenide (both 5×10^{-3} M) with 450 nm lamps.¹⁶

Minimum energy conformations were calculated using a Macintosh IIsi computer with a MM2 type force field as supplied in the Chem 3D software package.¹⁴ The calculations of electronic structure and optical spectra were performed using the semiempirical INDO/S-SCF-CI (ZINDO) algorithm developed by Zerner and co-workers.¹⁸ The ZINDO calculations were performed on a Stellar mini supercomputer and required approximately 5–10 min of CPU time.

Materials. All solvents were spectral grade (Aldrich or Fisher) unless otherwise noted. Dichloromethane was distilled over calcium hydride, and benzene was distilled over sodium metal prior to use. Cyclohexane, hexane, acetonitrile, ethyl alcohol (anhydrous, Aldrich), and dimethyl sulfoxide (HPLC grade, Aldrich) were used as received. *trans*-Stilbene (Aldrich) was recrystallized two times from benzene and once from ethyl alcohol. All other compounds were used as received unless otherwise indicated.

***trans*- and *cis*-Ethyl 3-(2-Indolyl)propenoate (*E-2* and *Z-2*).** Reduction of indole-2-carboxylic acid (Aldrich) with LiAlH₄ afforded 2-hydroxymethylindole [89%, mp 73–73.5 °C (lit²⁶ mp 75–76 °C)]. Oxidation of the alcohol using sodium dichromate dihydrate and concentrated sulfuric acid in DMSO²⁷ yielded 2-indolecarboxaldehyde [34%, mp 141.5–142.5 °C (lit²⁸ mp 139–141 °C)]. A salt-free Wittig reaction²⁸ of the aldehyde with (carbethoxymethylene)triphenylphosphorane (Aldrich) afforded a mixture of *E-2* and *Z-2* which was separated by column chromatography using benzene as eluent to provide *E-2* and *Z-2* (73% and 7%, respectively) as pale yellow solids of high purity ($> 99\%$ by GC analysis). *E-2*: mp = 121–122 °C; ¹H NMR (CDCl₃) δ 1.36 (t, $J = 7.1$ Hz, 3H), 4.30 (q, $J = 7.1$ Hz, 2H), 6.26 (d, $J = 16.1$ Hz, 1H), 6.83 (s, 1H), 7.15 (t, $J = 8.0$

Hz, 1H), 7.27 (t, $J = 8.2$ Hz, 1H), 7.39 (d, $J = 8.2$ Hz, 1H), 7.63 (d, $J = 8.0$ Hz, 1H), 7.69 (d, $J = 16.2$ Hz, 1H), 8.49 (bs, 1H); ^{13}C NMR (CDCl_3) δ 14.3, 60.6, 109.0, 111.1, 115.4, 120.6, 121.5, 124.6, 128.4, 133.3, 134.3, 137.7, 167.0; IR (CHCl_3) 3471, 1695, 1634, 1268, 1180, 1128 cm^{-1} ; MS (m/e) 215 (M^+ , 89), 169 (100), 141 (33), 115 (24), 89 (9); HRMS 215.0958 (obsd) and 215.0947 (calcd). Anal. Calcd for $\text{C}_{13}\text{H}_{13}\text{N}_2\text{O}$: C, 72.53; H, 6.09; N, 6.51. Found: C, 72.29; H, 6.12; N, 6.40. **Z-2**: mp = 84.5–85.5 °C; ^1H NMR (CDCl_3) δ 1.35 (t, $J = 7.1$ Hz, 3H), 4.27 (q, $J = 7.1$ Hz, 2H), 5.78 (d, $J = 12.6$ Hz, 1H), 6.76 (s, 1H), 6.93 (d, $J = 12.6$ Hz, 1H), 7.09 (t, $J = 7.1$ Hz, 1H), 7.26 (t, $J = 7.1$ Hz, 1H), 7.44 (d, $J = 8.1$ Hz, 1H), 7.62 (d, $J = 8.0$ Hz, 1H), 11.87 (bs, 1H); ^{13}C NMR (CDCl_3) δ 14.2, 60.8, 111.7, 112.0, 112.9, 120.1, 121.4, 124.7, 127.5, 133.7, 135.1, 137.6, 168.5; IR (CHCl_3) 3300, 1694, 1614, 1201, 1125 cm^{-1} ; MS (m/e): 215 (M^+ , 87), 169 (100), 141 (36), 115 (26), 89 (15); HRMS 215.0962 (obsd) and 215.0947 (calcd).

trans- and cis-Ethyl 3-(3-Methyl-2-indolyl)propenoate (E-3 and Z-3). 2,3-Dimethylindole (TCI) was converted to 3-methyl-2-indolecarboxaldehyde by the method of Sakai et al.²⁹ [21%, mp 137–139 °C (lit²⁹ mp 139 °C)]. Wittig reaction of aldehyde as described above followed by column chromatography provided **E-3** and **Z-3** (96% and 4%, respectively) as pale yellow solids of high purity (>99% by GC analysis). Irradiation of **E-3** in dichloromethane solution with 350 nm light afforded a 20:1 mixture of **Z-3**:**E-3** from which pure **Z-3** could be obtained by column chromatography followed by recrystallization. **E-3**: mp = 157–158 °C; ^1H NMR (CDCl_3) δ 1.34 (t, $J = 7.1$ Hz, 3H), 2.39 (s, 3H), 4.30 (q, $J = 7.1$ Hz, 2H), 6.20 (d, $J = 15.9$ Hz, 1H), 7.09 (t, $J = 7.1$ Hz, 1H), 7.22–7.36 (m, 2H), 7.56 (d, $J = 7.8$ Hz, 1H), 7.82 (d, $J = 15.9$ Hz, 1H), 8.58 (bs, 1H); ^{13}C NMR (CDCl_3) δ 8.9, 14.3, 60.0, 111.0, 113.7 (2C), 118.7, 119.8, 125.0, 129.0, 129.9, 132.3, 137.4, 167.4; IR (CHCl_3) 3478, 1689, 1626, 1284, 1179 cm^{-1} . **Z-3**: mp = 56.5–57 °C; ^1H NMR (CDCl_3) δ 1.37 (t, $J = 7.1$ Hz, 3H), 2.45 (s, 3H), 4.28 (q, $J = 7.1$ Hz, 2H), 5.77 (d, $J = 12.7$ Hz, 1H), 7.04–7.12 (m, 2H), 7.27 (t, $J = 7.0$ Hz, 1H), 7.41 (d, $J = 8.3$ Hz, 1H), 7.59 (d, $J = 8.1$ Hz, 1H), 11.80 (bs, 1H); ^{13}C NMR (CDCl_3) δ 9.1, 14.2, 60.7, 111.4 (2C), 111.8, 119.3, 119.8, 125.0, 127.8, 130.2, 132.1, 136.6, 168.8; IR (CHCl_3) 3300, 1688, 1599, 1336, 1191 cm^{-1} . Anal. Calcd for $\text{C}_{14}\text{H}_{15}\text{N}_2\text{O}$: C, 73.33; H, 6.60; N, 6.11. Found: C, 72.99; H, 6.58; N, 5.99.

trans- and cis-Ethyl 3-(N-Methyl-2-indolyl)propenoate (E-4 and Z-4). Methylation of **E-2** and **Z-2** by the method of Eenkhuom et al.³⁰ using sodium hydride as the base and methyl iodide as the methylating reagent in *N,N*-dimethylformamide afforded **E-4** and **Z-4** (55–60%). **E-4** was purified (>99% pure on the basis of GC analysis) by recrystallization from benzene/hexane and then by column chromatography using benzene as the eluent. **Z-4** was purified by column chromatography and then by preparative TLC using benzene as the eluent and the mobile phase. The resulting pale yellow oil contained ca. 2–3% impurity of **E-4**. **E-4**: mp = 87–87.5 °C; ^1H NMR (CDCl_3) δ 1.36 (t, $J = 7.1$ Hz, 3H), 3.83 (s, 3H), 4.29 (q, $J = 7.1$ Hz, 2H), 6.49 (d, $J = 15.7$ Hz, 1H), 6.96 (s, 1H), 7.12 (t, $J = 8.0$ Hz, 1H), 7.21–7.37 (m, 2H), 7.62 (d, $J = 8.0$ Hz, 1H), 7.80 (d, $J = 15.7$ Hz, 1H). ^{13}C NMR (CDCl_3) δ 14.4, 30.0, 60.6, 103.7, 109.6, 118.1, 120.4, 121.3, 123.6, 127.4, 132.6, 134.9, 139.0, 167.0. IR (CHCl_3) 1701, 1631, 1282, 1184 cm^{-1} . Anal. Calcd for $\text{C}_{14}\text{H}_{15}\text{N}_2\text{O}$: C, 73.33; H, 6.60; N, 6.11. Found: C, 73.30; H, 6.56; N, 6.15. **Z-4**: oil; ^1H NMR (CDCl_3) δ 7.66 (t, $J = 7.6$ Hz, 1H), 7.67 (s, 1H), 7.32–7.23 (m, 2H), 7.10 (t, $J = 7.9$ Hz, 1H), 6.97 (d, $J = 12.9$ Hz, 1H), 5.99 (d, $J = 12.8$ Hz, 1H), 4.26 (q, $J = 7.1$, 2H), 3.78 (s, 3H), 1.32 (t, $J = 7.1$, 3 Hz, 3H); ^{13}C NMR (CDCl_3) δ 165.9, 138.0, 133.2, 130.3, 127.4,

123.5, 121.9, 119.9, 118.2, 109.4, 108.2, 60.3, 29.7, 14.2; IR (CHCl_3) 1709, 1622, 1446, 1181 cm^{-1} .

trans-N,N-Dimethyl-3-(2-indolyl)propenamide (E-5). The ester **E-2** was converted to the amide **E-5** (72%) on standing for 3 days in a saturated methanolic solution of dimethylamine in the presence of sodium methoxide.³¹ mp = 234.5–235 °C; ^1H NMR (CDCl_3) δ 3.11 (s, 3H), 3.21 (s, 3H), 6.78 (d, $J = 15.6$ Hz, 1H), 6.81 (s, 1H), 7.11 (t, $J = 7.1$ Hz, 1H), 7.23 (t, $J = 7.1$ Hz, 1H), 7.37 (d, $J = 8.0$ Hz, 1H), 7.61 (d, $J = 8.0$ Hz, 1H), 7.76 (d, $J = 15.4$ Hz, 1H), 8.76 (bs, 1H); ^{13}C NMR (CD_3OD) δ 36.3, 37.8, 108.9, 112.1, 115.4, 120.8, 122.1, 124.9, 129.8, 134.2, 135.8, 139.7, 169.1. IR (CHCl_3) 3467, 1648, 1596, 1126 cm^{-1} ; MS (m/e) 214 (M^+ , 70), 170 (100), 142 (31), 115 (34), 89 (11); HRMS 214.1117 (obsd) and 214.1106 (calcd).

cis-N,N-Dimethyl-3-(2-indonyl)propenamide (Z-5). A 0.01 M solution of **E-5** in dichloromethane was irradiated in a Rayonet reactor fitted with RPR 3500 lamps. The photolysis was stopped after reaching the photostationary state consisting of ca. 96% cis isomer. The solvent was removed and the residue chromatographed on silica gel using hexane/ethyl acetate (1:1) eluent to provide the **Z-5** in >99% purity on the basis of GC analysis. Mp = 79–80 °C; ^1H -NMR (CDCl_3) δ 3.02 (s, 3H), 3.07 (s, 3H), 5.97 (d, $J = 12.7$ Hz, 1H), 6.61 (s, 1H), 6.75 (d, $J = 12.7$ Hz, 1H), 6.99 (t, $J = 7.9$ Hz, 1H), 7.14 (t, $J = 8.0$ Hz, 1H), 7.36 (d, $J = 8.3$ Hz, 1H), 7.52 (d, $J = 8.1$ Hz, 1H), 12.15 (bs, 1H); ^{13}C NMR (CDCl_3) δ 36.1, 38.4, 109.8, 112.0, 113.4, 119.7, 121.0, 123.9, 127.8, 131.5, 134.1, 137.4, 167.7; IR (CHCl_3) 3246, 1640, 1591, 1121 cm^{-1} ; MS (m/e) 214 (M^+ , 93), 170 (100), 142 (29), 115 (33), 89 (10); HRMS 214.1098 (obsd) and 214.1106 (calcd).

Acknowledgment is made to the donors of the Petroleum Research Fund, administered by the American Chemical Society, for support of this research.

Supporting Information Available: Figures S1–S3 showing symmetries and energies of frontier orbitals and Table S1 reporting calculated absorption maxima, oscillator strengths, and configuration interactions of the singlet states of *anti-E-2*, *syn-E-2*, and **Z-2** (4 pages). Ordering information is given on any current masthead page.

References and Notes

- Mazzucato, U.; Momicchioli, F. *Chem. Rev.* **1991**, *91*, 1679 and references cited therein.
- (a) Salties, J.; Choi, J.-O.; Sears, D. F., Jr.; Eaker, D. W.; Mallory, F. B.; Mallory, C. W. *J. Phys. Chem.* **1994**, *98*, 13162. (b) Shim, S. C.; Kim, D. W.; Kim, M. S. *J. Photochem. Photobiol. A.* **1991**, *56*, 227.
- (a) Arai, T.; Moriyama, M.; Tokumaru, K. *J. Am. Chem. Soc.* **1994**, *116*, 3171. (b) Arai, T.; Iwasaki, T.; Tokumaru, K. *Chem. Lett.* **1993**, 691.
- Lewis, F. D.; Yoon, B. A.; Arai, T.; Iwasaki, T.; Tokumaru, K. *J. Am. Chem. Soc.* **1995**, *117*, 3029.
- (a) Lewis, F. D.; Stern, C. L.; Yoon, B. A. *J. Am. Chem. Soc.* **1992**, *114*, 3131. (b) Lewis, F. D.; Yoon, B. A. *J. Org. Chem.* **1994**, *59*, 2537.
- (a) Lewis, F. D.; Yoon, B. A. *J. Photochem. Photobiol. A.* **1995**, *87*, 193. (b) Lewis, F. D.; Yoon, B. A. *Res. Chem. Intermed.* **1995**, *21*, 749.
- Gopal, V. R.; Reddy, A. M.; Rao, V. J. *J. Org. Chem.* **1995**, *60*, 7966.
- Tanaka, H.; Takamuku, S.; Sakurai, H. *Bull. Chem. Soc. Jpn.* **1979**, *52*, 801.
- Lewis, F. D.; Denari, J. M. *J. Photochem. Photobiol. A.* in press.
- Junge, H. *Spectrochim. Acta* **1968**, *24A*, 1965.
- (a) Lewis, F. D.; Elbert, J. E.; Uthagrove, A. L.; Hale, P. D. *J. Org. Chem.* **1991**, *56*, 553 and references cited therein. (b) Lewis, F. D.; Howard, D. K.; Oxman, J. D.; Uthagrove, A. L.; Quillen, S. L. *J. Am. Chem. Soc.* **1986**, *108*, 5964.
- Lambert, J. B. In *Conformational Analysis of Cyclohexenes, Cyclohexadienes and Related Hydroaromatic Compounds*; Rabideau, P. W., Ed.; VCH: New York, 1989; pp 47–63.
- Sanders, J. K. M.; Hunter, B. K. *Modern NMR Spectroscopy*; Oxford University Press: Oxford, England, 1987, Chapter 6.

- (14) Chem 3D Plus, Cambridge Scientific Computing, Inc.
- (15) Somewhat smaller energy differences for s-cis vs s-trans enone conformers were obtained using PC-MODEL (SERENA Software, Bloomington, IN). O. G. Dmitrenko, private communication.
- (16) (a) Yamashita, S. *Bull. Chem. Soc. Jpn.* **1961**, *34*, 972. (b) Ushakov, E. N.; Lednev, I. K.; Alfimov, M. V. *Dokl. Akad. Nauk. SSSR* **1990**, *313*, 903.
- (17) Fueno, T.; Yamaguchi, K.; Naka, Y. *Bull. Chem. Soc. Jpn.* **1972**, *45*, 3294.
- (18) (a) Bacon, A. D.; Zerner, M. C. *Theor. Chim. Acta.* **1970**, *53*, 21. (b) Zerner, M. C.; Loew, G. H.; Kirchner, R. R.; Mueller-Westerhoff, U. T. *J. Am. Chem. Soc.* **1980**, *102*, 589.
- (19) Lewis, F. D.; Salvi, G. D.; Kanis, D. R.; Ratner, M. A. *Inorg. Chem.* **1993**, *32*, 1251.
- (20) Vo-Dinh, T. *Mod. Fluoresc. Spectrosc.* **1981**, *4*, 167.
- (21) (a) Saltiel, J.; Eaker, D. W. *J. Am. Chem. Soc.* **1984**, *106*, 7624. (b) Fischer, G.; Fischer, E. *J. Phys. Chem.* **1981**, *85*, 2611.
- (22) Fischer, E. *J. Photochem.* **1981**, *17*, 331.
- (23) (a) Dawson, W. R.; Winsdor, M. W. *J. Phys. Chem.* **1968**, *72*, 3251. (b) Value from ref 23c adjusted according to: Meech, S. R.; Phillips, D. *J. Photochem.* **1983**, *23*, 193. (c) Berlman, I. B. *Fluorescence Spectra of Aromatic Molecules*; Academic: New York, 1971.
- (24) James, D. R.; Siemiarczuk, A.; Ware, W. R. *Rev. Sci. Instrum.* **1992**, *63*, 1710.
- (25) Lewis, F. D.; Johnson, D. E. *J. Photochem.* **1977**, *7*, 421.
- (26) Echavarren, A. M. *J. Org. Chem.* **1990**, *55*, 4255.
- (27) Shyamsunder Rao, Y.; Filler, R. *J. Org. Chem.* **1974**, *39*, 3304.
- (28) Pindur, U.; Eitel, M. *Synthesis* **1989**, 364.
- (29) Sakai, S.-I.; Kubo, A.; Katsuura, K. *Chem. Pharm. Bull.* **1972**, *20*, 76.
- (30) Eenkhorn, J. A.; de Silva, S. O.; Snieckus, V. *Can. J. Chem.* **1973**, *51*, 792.
- (31) Stella, L.; Raynier, B.; Surzur, J. M. *Tetrahedron Lett.* **1977**, 2721. JP960907C